

# Comparative analysis of contributing parameters for rainfall-triggered landslides in the Lesser Himalaya of Nepal

Netra Bhandary

*Environmental Geology*

## Cite this paper

Downloaded from [Academia.edu](#) 

[Get the citation in MLA, APA, or Chicago styles](#)

## Related papers

[Download a PDF Pack](#) of the best related papers 



[Engineering Geology and Stability of the Laprak Landslide, Gorkha District, Western Nepal](#)  
R. Gunturi

[A study on socio economic effects of landslides in Iran](#)  
Emad Osman, reza bagherian

[Slope stability analysis on a regional scale using GIS: a case study from Dhading, Nepal](#)  
Prithvi Pathak

# Comparative analysis of contributing parameters for rainfall-triggered landslides in the Lesser Himalaya of Nepal

Ranjan Kumar Dahal · Shuichi Hasegawa ·  
Minoru Yamanaka · Santosh Dhakal ·  
Netra Prakash Bhandary · Ryuichi Yatabe

Received: 19 November 2007 / Accepted: 20 August 2008  
© Springer-Verlag 2008

**Abstract** In the Himalaya, people live in widely spread settlements and suffer more from landslides than from any other type of natural disaster. The intense summer monsoons are the main factor in triggering landslides. However, the relations between landslides and slope hydrology have not been a focal topic in Himalayan landslide research. This paper deals with the contributing parameters for the rainfall-triggered landslides which occurred during an extreme monsoon rainfall event on 23 July 2002, in the south-western hills of Kathmandu valley, in the Lesser Himalaya, Nepal. Parameters such as bedrock geology, geomorphology, geotechnical properties of soil, and clay mineralogy are described in this paper. Landslide modeling was performed in SEEP/W and SLOPE/W to understand the relationship of pore water pressure variations in soil layers and to determine the spatial variation of landslide occurrence. Soil characteristics, low angle of internal friction of fines in soil, medium range of soil permeability, presence of clay minerals in soil, bedrock

hydrogeology, and human intervention were found to be the main contributing parameters for slope failures in the region.

**Keywords** Rainfall-triggered landslides · Himalaya · Clay minerals · Seepage analysis · Stability analysis

## Introduction

The Himalayan mountain chain measures 2,400 km in length and is one of the most active and fragile mountain ranges on the earth. Landslides are very common in the Himalayan terrain, and intense summer monsoons are the main landslide-triggering factor. Every year, especially during monsoon periods, extensive damage to lives, property, infrastructure, and environment in the Himalayan country of Nepal is caused by landslides and related natural events. The annual economic losses due to landslide damages alone in the Himalayan region are estimated to exceed 1 billion US dollars, including hundreds of human fatalities. Studies have indicated that the losses due to landslides and related problems in the Himalayan region alone constitute about 30% of the world's total landslide-related damage value (Li 1990). In Nepal, people live in widely spread settlements in the fragile Himalayan terrains, and suffer more from the landslides than any other types of natural disasters. A large number of human settlements on the Nepalese mountains and hills are situated either on old landslide masses or on landslide-prone areas. Because of this, a great number of people are affected by large- and small-scale landslides all over the Nepal, especially during monsoon periods. For example, in only half of the 2008 monsoon period (i.e., from 10 June–15 August), 50 people were killed by landslides (NRCS 2008, unpublished).

---

R. K. Dahal (✉) · S. Hasegawa · M. Yamanaka  
Department of Safety Systems Construction Engineering,  
Faculty of Engineering, Kagawa University, 2217-20,  
Hayashi-cho, Takamatsu 761-0396, Japan  
e-mail: ranjan@ranjan.net.np  
URL: www.ranjan.net.np

R. K. Dahal  
Department of Geology, Tri-Chandra Multiple Campus,  
Tribhuvan University, Ghantaghar, Kathmandu, Nepal

S. Dhakal  
Department of Mines and Geology, Lainchaur,  
Kathmandu, Nepal

N. P. Bhandary · R. Yatabe  
Department of Civil and Environmental Engineering,  
Ehime University, Bunkyo-3, 790-8577 Matsuyama, Japan

To date, most Himalayan landslide research has concentrated on loss of lives and wealth, physical properties of landslides and debris flows, effect of regional and local geological settings, and recommendations for environmentally friendly mitigative measures (Wagner 1983; Dhital et al. 1993; JICA 1993; Upreti and Dhital 1996; Dhital 2003; Hasegawa et al. 2008). Similarly, recent work by Dahal and Hasegawa (2008) established the rainfall threshold for landslides in the Nepal Himalaya. Still, the relationship between landslides and slope hydrology as well as the strength of slope materials has not been a focal topic in Himalayan landslide research owing to limited number of researchers involved in this area of study. In this context, the current paper attempts to deal with some of the crucial hydrological and geotechnical issues of shallow landslides in the Lesser Himalaya of central Nepal.

There have been many studies that illustrate the general and numerical relationships between landslides and rainfall in various regions such as the Alps and Rockies as well as Japan and humid tropical regions. Some studies show that the type of rainfall-triggered landslide depends largely upon intensity and duration of rainfall (Campbell 1975; Caine 1980; Brand et al. 1984; Wieczorek 1987; Wilson and Wieczorek 1995; Crozier 1999; Guzzetti et al. 2004; Aleotti 2004; Giannecchini 2006; Dahal and Hasegawa 2008). Studies have shown that both deep- and shallow-seated landslides can be triggered by rainfall, but deep-seated landslides are triggered by rainfall over extended periods with a moderate intensity, while shallow landslides such as soil slips and debris flows are usually triggered by short duration, intense precipitations. Different approaches have been presented to explain the relationship between rainfall and slope failures in terms of rainfall thresholds, hydrological models, and coupled hydrological and stability models (Hungri 1995; Borga et al. 2002; Rezaur et al. 2002; Rahardjo et al. 2002; Tsaparas et al. 2002; Dhakal and Sidle 2004; Kim et al. 2004; Dahal et al. 2008a; Rahardjo et al. 2005; Tofani et al. 2006). Rainfall and liquefaction of slope materials have also been examined recently (Anderson and Sitar 1995; Montgomery et al. 1997; Sassa 1998; Dai et al. 1999; Lan et al. 2003; Collins and Znidarcic 2004; Cai and Ugai 2004) and it is generally observed that rainfall-triggered landslides in coarse grained soils are caused by increased pore pressures and seepage forces during periods of intense rainfall. In contrast, fine grained soils with low infiltration rates do not lead to the development of positive pore pressure, and failures occur due to a decrease in the shear strength of soils caused by the loss of matric suction. Likewise, studies have also suggested that shallow failures are usually associated with increased positive pore water pressure, while loss of negative pore water pressure or matric suction is mainly responsible for deep-seated failure. The mobilization of

debris flows from slides has also been studied (Ellen and Fleming 1987; Iverson 1997; Iverson et al. 1997; Olivares and Picarelli 2003), and it has been observed that liquefaction of slope materials plays a key role in debris-flow initiation and motion.

A realistic understanding of the distribution of pore water pressures, both positive and negative, is fundamental in rainfall-triggered landslide studies and modeling (Rahardjo et al. 1995). Monitoring results have indicated a highly variable distribution of pore water pressures during intense rainfall events in colluvial soils (Fannin and Jaakkola 1999). This is mostly due to the varying characteristics of slope materials concerning the degree of weathering, rock joints, and hydraulic conductivity. Hydrological models have typically been used to simulate saturated and unsaturated flow in slopes. The hydrological models can be linked to slope stability models to enable accurate simulations of the conceivable slope stability conditions during rainfall. HYSWASOR (Van Genuchten 1980) and Combined Hydrology and Slope Stability Model (CHASM) (Anderson and Lloyd 1991; Collison and Anderson 1996) are the two examples of such hydrological models. A successful approach to modeling the influence of topography on slope material saturation behavior was established by Beven and Kirkby (1979), in the form of a topography index. This model was incorporated successfully into a hydrological model known as TOPMODEL, which simulated runoff hydrographs (Lamb et al. 1998). Dietrich et al. (1995) and Montgomery and Dietrich (1994) developed a contour- or polygon-based hill slope hydrological model called SHALSTAB. This model also considered some of the index properties of slope materials, and can be implemented as an extension of commercially available GIS software (ArcView). Pack et al. (1998, 2001) developed another approach (SINMAP), which is suitable for modeling slopes that have a shallow soil depth and impermeable underlying bedrock. It is similar to SHALSTAB, but uses cohesion and root cohesion (for forested slopes) in the calculations. Thus, SINMAP may be viewed as an advanced version of SHALSTAB. The contributing area is one of the important topographic parameters used in SINMAP. The model described by Iverson (2000) illustrates the infiltration process of rainfall and landslide processes. He showed that the use of pressure head response, topographic data, rainfall intensity and duration, along with infinite-slope failure criteria, helps to predict the timing, depth, and acceleration of rainfall-induced landslides. The Antecedent Soil Water Status Model (ASWSM) described by Crozier (1999) and Glade et al. (2000) accounted for the draining of early rainfall and accumulation of late rainfall. They provided an equation for estimating the probability of landslide occurrence as a function of daily intensity and previous water accumulation.

The GeoStudio package (GeoStudio 2005) is another example of a coupled hydrological-slope stability modeling software. The SEEP/W (GeoStudio 2005) of the GeoStudio package analyses seepage problems with a numerical discretization technique, whereas SLOPE/W can be used as a limit equilibrium slope stability model. SEEP/W adopts an implicit numerical solution to solve Darcy's equation for saturated and unsaturated flow conditions, describing pore water pressure and movement patterns within porous materials over space and time. Coupled SEEP/W–SLOPE/W analyses (Krahn 2004a, b) have been employed successively to evaluate dynamic stability conditions of embankments and slopes (Rinaldi and Casagli 1999; Crosta and Dal Negro 2003; Rinaldi et al. 2004; Collins and Znidarcic 2004; Dapporto et al. 2005). The results obtained from seepage modeling can be directly linked into SLOPE/W, and it uses a variety of methods to solve problems for the factor of safety (GeoStudio 2005). The literature shows that a wide range of contributing parameters can be involved in rainfall-induced landsliding process. Slope geomorphology, micro climate, bedrock structures, bedrock hydrology, saturated and unsaturated strength of the slope materials, clay mineralogy of slope materials, transient pore water pressure development, and abrupt loss of strength are the main factors found to be responsible for rainfall-triggered landsliding processes.

### Objectives of the research

The main objective of this study was to investigate the contributing parameters responsible for rainfall-triggered landsliding in the Lesser Himalaya. For this purpose, a rainfall-triggered landslide event which occurred during an extreme monsoon rainfall on 22–23 July 2002, in the south-western hills of Kathmandu valley, Lesser Himalaya, central Nepal was selected for study. Although the event triggered over 73 landslides in the south-western hills of Kathmandu valley, only the central part (Matatirtha area) and most affected area was chosen for study. There were a total of 12 landslides and debris flows in the Matatirtha area. One soil slide with debris flow, which is referred as the Matatirtha landslide in this paper, killed 16 people and destroyed six houses (Dahal et al. 2006). There are two ridges in the selected area but only one ridge (ridge of the Matatirtha landslide) is highly affected by landslides, although both have similar geological and geomorphological settings. Thus the site was evaluated in terms of geomorphology, bedrock hydrogeology, and slope material strength with groundwater seepage and slope stability modeling. The detailed objectives of this research can be explicitly listed as follows:

- to explore the role of geological and geomorphological setting and their spatial variation on landsliding,
- to understand the effectiveness of bedrock joints for groundwater flow during landsliding,
- to discover the spatial variation of seepage in accordance with soil hydraulic conductivity and other physical properties, and
- to outline the contributing parameters for landsliding by comparing non landslide zones and landslide-prone zones.

### The study area

#### Location and geology

The study area is located in the south-western hills of the Kathmandu valley, Nepal (Fig. 1). The Kathmandu valley is an intermountain basin that is surrounded by high rising mountain ranges, such as Shivapuri (2,732 m) in the north, Phulchowki (2,762 m) in the southeast, and Chandragiri (2,543 m) in the southwest.

The study area is within the Lesser Himalaya and situated close to the central part of Nepal. The basement rock consists of the rocks of the Phulchauki Group (Stöcklin 1980) and is comprised of weakly metamorphosed sediments of early to middle Paleozoic age. Limestone and a subordinate amount of shale and sandstone are main rock types of the study area (Fig. 2).

The altitude of the Matatirtha area ranges from 1,400 to 1,900 m, and colluvial soil is the main slope material above the bedrock. Until 20 years ago, the area was critically deforested, but since then the area has been reforested and is protected by the local communities. However, the newly planted trees are still not mature; at present, the area consists mainly of a dense forest of immature trees and thorny shrubs. The area is on the outskirts of Kathmandu Metropolitan city, and settlement at the base of the hills has risen sharply over the last 10 years. Because of the panoramic view of the Himalayas to the north, many housing projects have been started on the base of the hills without the consideration of landslide hazards.

Some research has been conducted in the study area. Paudel et al. (2003) described a disaster management scenario for the central part of the study area, giving examples of the disastrous landslides of 2002. Dahal and Kafle (2003) and Dahal et al. (2006) reported geological and geomorphological aspects of the Matatirtha landslide. Paudyal and Dhital (2005) used the InfoVal method to perform a statistical analysis of landslide hazard for the southern part of Kathmandu, including the study area, and categorized the levels of risk as low, moderate, and high.

**Fig. 1** Location map of southern hills of Kathmandu valley and the study area

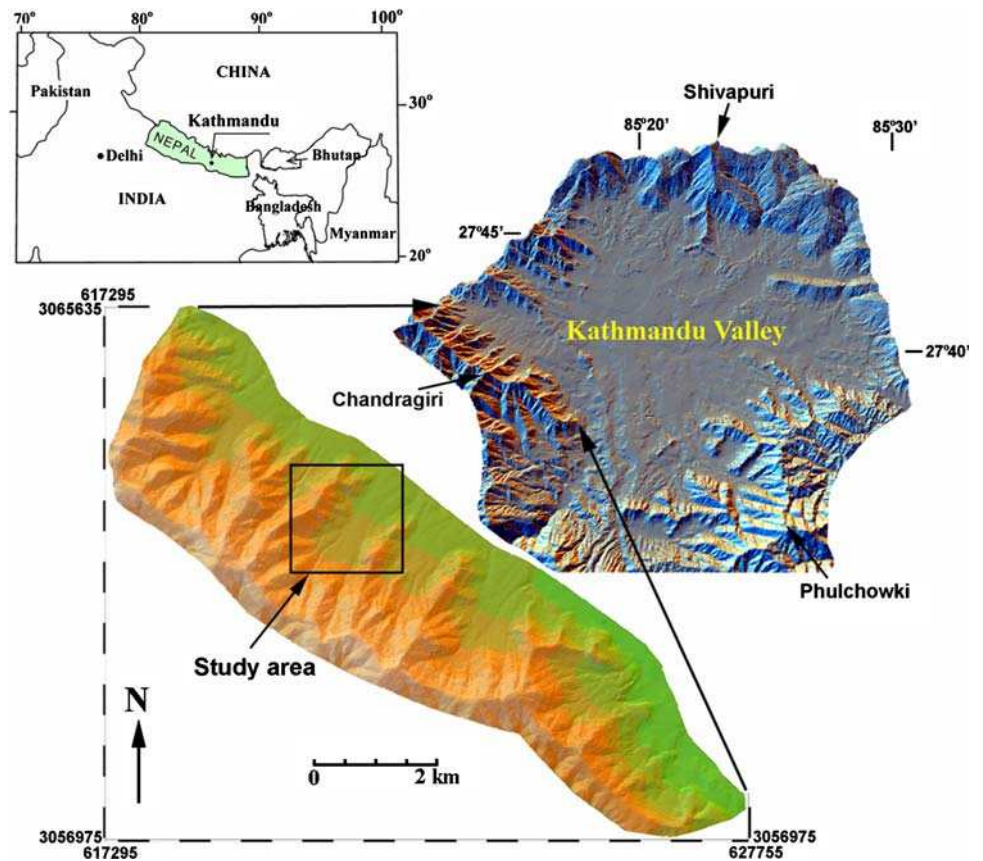
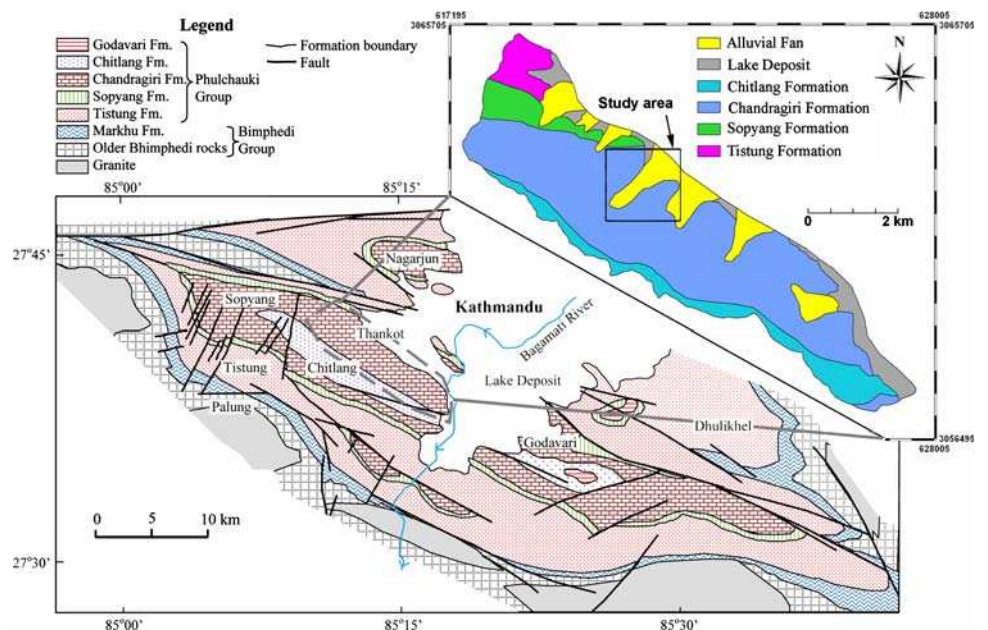


**Fig. 2** Geological map of Kathmandu area (modified after Stöcklin and Bhattarai 1977) and geological map of the southern hills of Kathmandu



Dahal et al. (2006) provided a comprehensive description of the study area with respect to the issue of rainfall and landslides. Dahal et al. (2008b, c) performed deterministic and statistical landslide hazard studies of the southern hills of Kathmandu including the study area, and categorized the levels of landslide hazard.

### Rainfall

From the meteorological point of view, the month of July is very critical for the study area. Plotting the last 34 years rainfall data at Thankot (Fig. 3) reveals that month of July of every year has the maximum rainfall. From 1 to 22 July

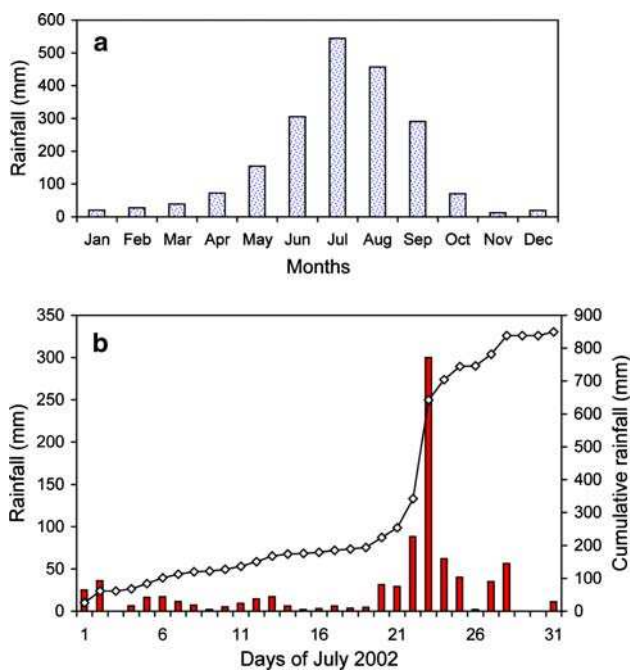


**Fig. 3** a Trend of monthly rainfall distribution of last 34 years (1970–2004) in study area and the monthly rainfall distribution is in approximately bell-shaped symmetric fashion with peak value in July. b Rainfall distribution of July 2002

2002, there was intermittent rainfall in the study area; the accumulated precipitation in southwest Kathmandu city for that period was approximately 342 mm, which is a little higher than the maximum 1 day rainfall (300.1 mm) on 23 July 2002 (Fig. 3). The rain gauge station is situated at Thankot, located at about 2 km north–west aerial distance from the study area and is not an automatic gauging station. Rainfall is manually measured everyday at 8:45 a.m. The rainfall amount of 300.1 mm on 23 July 2002 was also measured at 8:45 a.m. Most of the landslides in southern hills of Kathmandu occurred between 1:00 and 5:00 a.m. of 23 July 2002, and rainfall was almost stopped after 6:00 a.m. Thus, although there were no hourly rainfall data to correlate the exact rainfall amount and times of failure, the total daily rainfall amount recorded at 8:45 a.m. could also help to correlate the landslide events and rainfall.

**Geomorphological setting**

Physiographically, the area falls into the Midlands of the Lesser Himalaya (Upreti 1999). The selected area consists of two ridges, referred to as Matatirtha and Dhaksi ridges in this paper (Fig. 4). Matatirtha ridge consists of many landslides, including the Matatirtha landslide, whereas Dhaksi ridge does not have any landslides. The ridges are less than 1 km apart, are of similar elevation, and have the same types of vegetation, rocks, and soils. Both are elongated toward north from a main ridge to the south (Fig. 4).

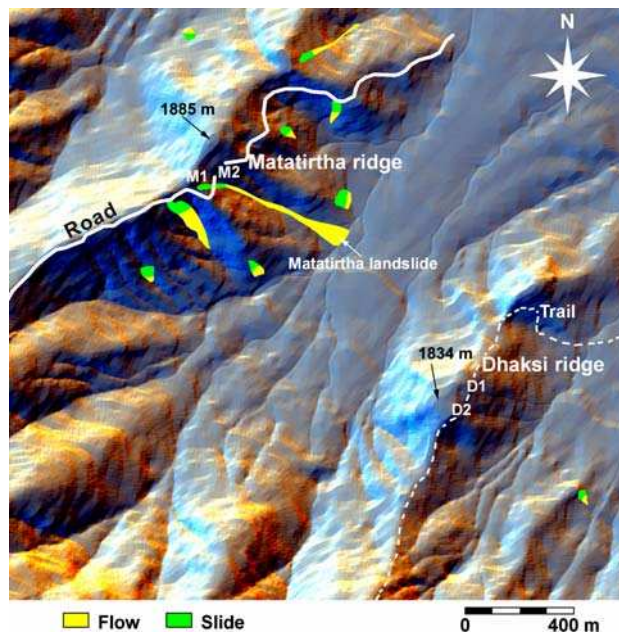


**Fig. 4** DEM image of the study area

Average elevation of both ridges is 1,840 m. The western parts of both ridges is relatively rockier than the eastern parts, and consist of rocky cliffs and less soil cover than the eastern parts.

For the detail geotechnical study and seepage analysis, four representative sites (M1, M2, D1, and D2) on the two ridges were selected (Fig. 4). Site M1 was located in the crown part of the Matatirtha landslides and M2 was in the upstream portion of a gully in which the debris flow occurred after failure at site M1 (Fig. 5a). Sites D1 and D2 were situated on zero-order basins (Tsukamoto et al. 1982; Tsuboyama et al. 2000) on Dhaksi ridge (Fig. 5b). Downslope of both sites consists of prominent first order gullies. The zero-order basins at sites M1 and M2 are a little wider than sites D1 and D2. The locations for the geotechnical investigations were selected according to the fact that soils of zero-order basins are usually more prone to slope failure than the soil in surrounding ridges (Dunne 1978; Hennrich and Crozier 2004). Matatirtha ridge has an old earthen road (width 3.5 m) passing through the entire ridge, whereas Dhaksi ridge also has an old trail (average width 2 m) which also crosses location D1 and D2.

**The disastrous Matatirtha landslide**

From the preliminary field investigation and mapping of landslides on Matatirtha ridge immediately after the disasters, it was noticed that all of the debris flows in the study area possessed the same characteristics. All landslides had a small slide in the source area and then the displaced soil mass grew in volume while moving down

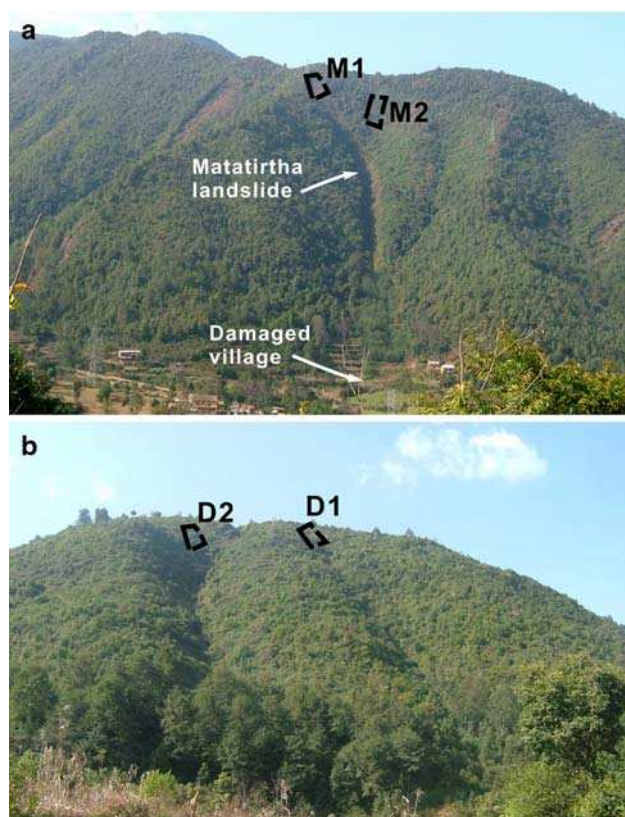


**Fig. 5** **a** Oblique view of Matatirtha ridge and location of selected sites M1 and M2 for geotechnical study and seepage analysis. **b** Oblique view of Dhaksi ridge and selected sites, D1 and D2, for geotechnical study and seepage analysis. View is toward west for both photographs

slope along a streambed, which usually had a very small catchment. Among these slope failures, the Matatirtha landslide, which occurred at about 3:45 a.m. on 23 July 2002, was the most typical in nature. Figure 6a shows an oblique view of the Matatirtha landslide taken 32 h after the events and Fig. 6b is a plan view of the landslide. In both figures, it can be noticed that the landslide occurred on the southern part of a concave slope or zero-order basin. This steep and vegetated zero-order basin consists of 1.0–2.1 m thick colluvial soil above the bedrock and failure occurred at contact between soil and rock. The failure initiated at the southern part of the gully (elevation 1,870 m) as debris slide, and failed materials accumulated and moved down along a gully which finally eroded all materials in its path and hit the settlement at the gully mouth. The flow initiated after accumulation of debris in the gully ended at about 1,570 m, damaging houses in its path. The colluvium which first detached from zone I (Fig. 6b) scraped off similar types of colluvial soil in zone II during its flow downslope. As a result, the volume of the moving material was increased by the integration process. Such process of integration is also known as bulking, and

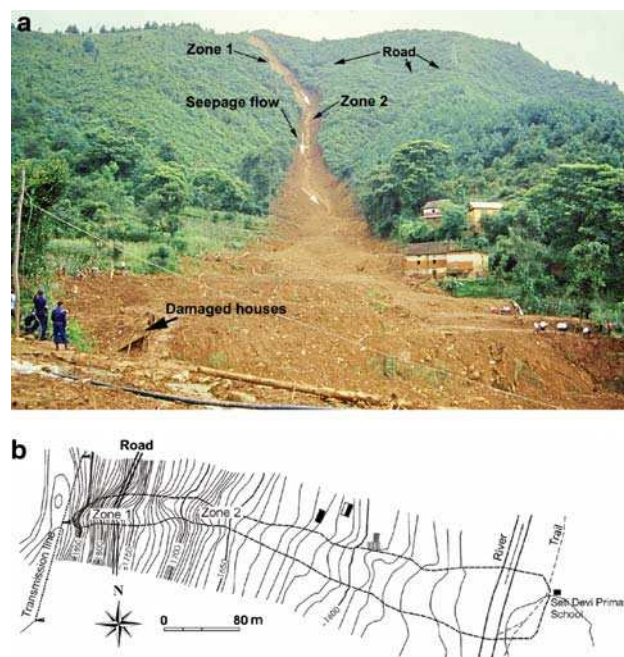


**Fig. 6** **a** Oblique view of Matatirtha landslide 32 h after landsliding. Seepages through rock were also seen, view from east to west. **b** Topographical map of landslide

has been reported by many researchers in other parts of the world (De Prete et al. 1998; Guadagno et al. 1999; Wang et al. 2003; Hungr 2003). Distance from crown to toe was measured as 552 m during the topographical survey. The uppermost part of zone I was estimated to be approximately 20.2 m wide and a maximum of 2.1 m deep. The distance from the crown to first 40.2 m length of slope in zone I is also relatively gentle ( $34^\circ$ ) and the average slope inclination is  $42^\circ$ . On the relatively gentle slope, average soil thickness is 1.46 m, whereas on steep slope the average soil thickness is less than 1 m. Soil thickness in zone II is also variable. In general, the upper reaches of the entire gully has thin colluvial soil deposits (less than 2 m) and the lower reaches have average thicknesses of 5.5 m.

Matatirtha ridge has an old earthen road that passes 43.5 m below the failure scar of the Matatirtha landslide (Figs. 4, 6a, b). This road is the tentative boundary between zones I and II. The road portrayed a state of toe cutting for zone I, and contributed as one of the failure parameters during rainfall. Most of the landslides on Matatirtha ridge are concentrated along this road (see Fig. 4).

Dahal and Kafle (2003) and Paudel et al. (2003) estimated the velocity and volume of materials involved in the Matatirtha landslide. Both used energy line and law of conservation of energy to calculate the velocity of the debris flow. They estimated the maximum velocity of the debris flow to be 40 m/s. Dahal and Kafle (2003) divided the landslide into two failure zones and calculated the

volume of displaced materials using total area and average depth of the slope materials. They suggested that a total of 8,960 m<sup>3</sup> of debris was involved in the Matatirtha landslide and that the yield rate (Hungri et al. 1984; Hungri 2003) of the landslide was about 20.6 m<sup>3</sup>/m in the uphill section and about 63.6 m<sup>3</sup>/m in the down slope gully. The down slope yield rates support the widened gully that resulted from the landslide. Paudel et al. (2003) estimated about 9,000 m<sup>3</sup> of material was involved in the landsliding.

## Investigation methodology

### Field investigations

A total of eight field visits and observations as well as measurements were carried out in the study area. The first preliminary field observations in the study area were performed 32 h after the main landslide events. In that time, disaster rescue teams were trying to recover dead bodies from the debris and buried houses. The first visit was very helpful to plan the research on the landslide and associated hazard in the study area.

In the initial phase, a topographical map of the area (scale 1:10,000) was used to prepare a landslide inventory map. The area was also regularly visited in 2003, 2004, 2005, and 2006 to observe the change in vegetation and response of other parts of the slopes during other monsoon rainfalls. The site was visited in winter of 2002 and a detailed geological study was carried out. A topographical survey was also carried out along the Matatirtha landslide gully, which helped to delineate the landslide boundary properly. Soil thickness along the debris flow path was also recorded during the field survey. Although weathered debris was exposed at lower altitudes, most of the newly exposed surface along the gully of the Matatirtha landslide consisted of bedrock, and colluvium that had been previously deposited by sliding, falling, or creeping of the weathered colluvium of the uphill section. Seepage locations were also noticed in later visits in 2003–2006.

### *In situ tests and soil sampling*

The main factor triggering the Matatirtha landslide was extreme rainfall. Thus, infiltration properties of the soil need to be understood for discussions of the hydrological characteristics of slope materials. Thus, to measure water infiltration rates of the soil, in situ infiltration tests were performed. The locations of the infiltration tests are already given in Figs. 4, 5 (M1 and M2 on Matatirtha ridge and D1 and D2 on Dhaksi ridge). On both ridges, slope inclination increases abruptly down slope from the location of the infiltration tests.

A double ring infiltrometer (ASTM D3385-03 2003) was used to determine saturated infiltration rates. Soil samples were also collected for soil classification, clay mineral identification, and identification of strength parameter in the lab. Tubes (100 cc) were used to collect samples for determining bulk density. Some soil samples were also collected from selected sites to understand the spatial variation of geotechnical properties of the slope materials.

### Rock fracture and ground water flow study

Detailed measurement of rock joints were carried out on both ridges to get information about rock fractures. A rock mass study template was prepared and completed in the field. Spacing of discontinuities, roughness of discontinuities, ground water flow, discontinuity length, aperture or separation, infilling materials, and weathering grade were recorded. The position of seepage and ground water flow locations were also noted.

### Experimental investigations

Soil samples collected from all four locations (M1 and M2 on Matatirtha ridge and D1 and D2 on Dhaksi ridge, see Figs. 4, 5) were investigated in the lab for index property identification, clay mineral studies, and strength parameter studies. All index parameters such as specific gravity, density, liquid limit, and plastic limit were determined in the lab along with the grain size distribution. Due to considerable amounts of rock fragments and sand in the soil, obtaining undisturbed samples for strength tests was not possible. Thus, direct shear and ring shear test were conducted in reconstituted soil specimens. Similarly, X-ray analyses were also carried out for study of the clay minerals.

A Bishop type (Bishop et al. 1971) ring shear apparatus was used for ring shear tests. The ring shear apparatus is capable of shearing a soil sample up to an infinitely large shear deformation without changing the area under shear (Bishop et al. 1971; Lupini et al. 1981; Stark and Eid 1994; Sassa 1998; Tika and Hutchinson 1999; Bhandary and Yatabe 2007; Wang et al. 2007). During the ring shear tests, all collected soil samples were sieved through a 425 µm sieve and mixed with water to make muddy liquids. Tests on each sample were conducted under two effective pressures, 98.1 and 196 kN/m<sup>2</sup> (1 and 2 kgf/cm<sup>2</sup>), considering the cohesion of reconsolidated saturated soil is zero. There was also the possibility of mechanical friction at high stress conditions, so the tests were conducted under comparatively lower stress conditions.

Similarly, as ring shear was conducted in the remolded and reconsolidated fine fraction of soils (<425 µm) under

saturated conditions, the tests could not provide the cohesion intercept. Thus, to estimate the effective cohesion and strength of the soils, box type direct shear tests were conducted. For site M1, a soil sample collected from the landslide scar was used for direct shear, whereas in the non-landslide sites, soil samples were collected from an average depth of 50 cm. The soil sample was reconstituted with sieved material finer than 2 mm to eliminate large fragments that could have altered the measurements. The applied normal loads ranged between 100 and 300 kN/m<sup>2</sup>.

X-ray diffraction analysis was employed to identify the constituent minerals of the collected soil samples. The powder method was used for the X-ray diffraction analysis, in which all particles were crushed into fine powder and constituent minerals were identified using X-ray diffraction patterns. The ethylene glycol treatment method was used to confirm the clay minerals of low values of 2θ (less than 15°).

### Analytical investigations

Understanding the distribution of pore water pressures, both positive and negative, is fundamental in rainfall-triggered landslide studies. Therefore, to analyze the variation of pore water pressure and slope instability in the selected sites (Figs. 4, 5), modeling of transient pore water pressure and slope stability was performed with finite element method (FEM) based computer applications such as SEEP/W and SLOPE/W (GeoStudio 2005). Modeling parameters were obtained from both field and laboratory investigations. The model code is based upon the equations of motion and mass conservation. Both saturated and unsaturated flows are simulated using a modified version of Darcy’s law. For unsaturated conditions, the hydraulic conductivity function is described by the relationship between water content and pore water pressure (Fredlund and Rahardjo 1993). In the case of transient flow, the hydraulic head is no longer independent of time and volumetric water content changes with time. Thus, Richard’s equation needs to be adopted for describing transient flow (Richards 1931; Fredlund and Rahardjo 1993) as follows:

$$\frac{\partial}{\partial x} \left( k_x \frac{\partial H}{\partial x} \right) + \frac{\partial}{\partial y} \left( k_y \frac{\partial H}{\partial y} \right) + q = \frac{\partial \theta}{\partial t} \quad (1)$$

where  $H$  is total head,  $k_x$  is hydraulic conductivity in the  $x$ -direction,  $k_y$  is hydraulic conductivity in the  $y$ -direction,  $q$  is applied boundary flux,  $\theta$  is volumetric water content, and  $t$  is time.

The state of stress and soil properties influence the change in the volumetric water content of soil, and the state of stress for both saturated and unsaturated conditions are usually described as  $\sigma - u_a$  and  $u_a - u_w$  (Fredlund and Morgenstern 1976, 1977; Fredlund and Rahardjo 1993).

The parameter  $\sigma$  is the total stress,  $u_a$  is the pore air pressure, and  $u_w$  is the pore water pressure. SEEP/W v.4 assumes that the pore air pressure remains constant at atmospheric pressure during transient flow. Hence,  $\sigma - u_a$  does not influence the changes in volumetric water content; rather, the stress variable  $u_a - u_w$  is responsible for changes in volumetric water content. When considering  $u_a$  as constant variable, the change in volumetric water content solely depends on the pore water pressure changes. As a result, the change in volumetric water content can be related to a change in pore water pressure and the right hand side of Eq. 2 can be written in the form of slope of the soil–water characteristics function (relation between the volumetric water content and the negative pore water pressures) as follows (Fredlund and Rahardjo 1993; Tsaparas et al. 2002):

$$\frac{\partial \theta}{\partial t} = m_w^2 \frac{\partial u_w}{\partial t} = m_w^2 \rho_w g \frac{\partial H}{\partial t} \quad (2)$$

where  $m_w^2$  is the coefficient of volumetric water change with respect to a change in negative pore water pressure, i.e., soil suction ( $u_a - u_w$ ) and is equal to the slope of the soil–water characteristic curve,  $\rho_w$  is the density of water, and  $g$  is gravitational acceleration.

Combining Eqs. 1 and 2, the final form of the governing equation of water flow through the unsaturated soil can be expressed as follows:

$$\frac{\partial}{\partial x} \left( k_x \frac{\partial H}{\partial x} \right) + \frac{\partial}{\partial y} \left( k_y \frac{\partial H}{\partial y} \right) + q = m_w^2 \rho_w g \frac{\partial H}{\partial t} \quad (3)$$

Equation 4 is an explicitly non-linear equation and SEEP/W uses finite elements to solve it. For the numerical solution of Eq. 4 in SEEP/W, it is necessary to provide the permeability function (permeability with respect to water versus negative pore water pressure), soil–water characteristic curve, boundary flux, and initial hydraulic head in the course of defining the problem.

## Results of field and laboratory investigations

### Geotechnical characteristics of soils

In situ and laboratory tests allowed the reconstruction of the mechanical behavior of the soils involved in the landslides. The stratigraphy at the four selected sites on Matatirtha and Dhaksi ridges includes homogenous colluvial soil and bedrock. In all landslides on Matatirtha ridge, failure surfaces were found to be localized on the contact between the colluvium and bedrock. The grain size distribution curves of the soils are shown in Fig. 7. Unified soil classification of the soil shows that the soil type of the selected sites is mainly silty clay of low plasticity (ML)

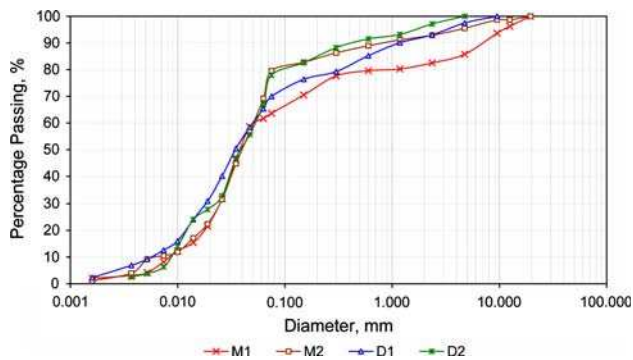


Fig. 7 Grain size distribution of soils of selected sites

with a considerable amount of sand and gravel (Figs. 7, 8). Soils from all four sites have nearly 60% fine materials and their grain size distribution curves are more or less similar.

Figure 9 shows a comparison of angles of peak and residual shear resistances of soils calculated from ring shear tests. The fine fraction of soils from Matatirtha ridge has considerably less residual strength than that from Dhaksi ridge. The effective friction angle (estimated from the box type direct shear test) of soils collected from sites M1 and M2 was also less than from sites D1 and D2. The ranges in Fig. 9 show that the peak angle of shear resistance varies between 18° and 36° on Dhaksi ridge and 12°–18° on Matatirtha ridge, whereas the residual angle of shear resistance varies between 16° and 36° on Dhaksi ridge and 10°–16° on Matatirtha ridge. Thus, the Dhaksi ridge soils have higher strength than Matatirtha ridge soils.

The results of the X-ray diffraction tests are provided in Table 1. From the X-ray diffraction patterns, it is clear that the main constituent minerals of the samples are quartz, feldspar, illite, chlorite, and smectite. Clay minerals having mixed layers of smectite and chlorites were also noticed.

The high intensity in X-ray diffraction patterns corresponding to illites indicates that the soils of the study area consist of a higher percentage of illites (also known as hydrous mica). Illites are mica and have thin sheet like structures, and have very low frictional resistance. Therefore, fine soil particles collected from sites M1 and M2 possess low value of angle of internal friction.

Bedrock hydrogeology

The rockmass study revealed three sets of joints. The bedding joint 219°/42° (dip direction/dip) was the major joint set. In most cases, joint separation was less than 1 mm without filling materials. However, some solution structures in limestone were noticed along the joints, which made the joint aperture more than 5 mm. Joint spacing in most of the cases was less than 0.5 m, and joint surfaces were slightly smooth. According to weathering grade

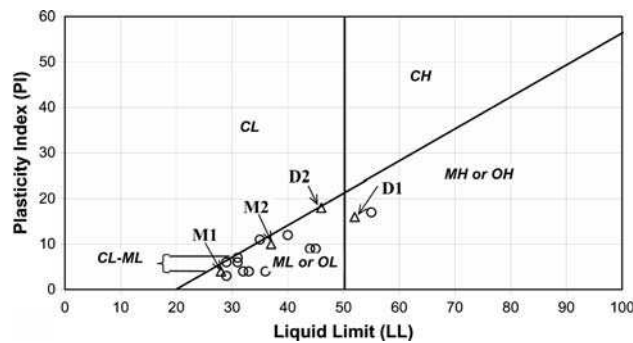


Fig. 8 Casagrande plot of Atterberg limits of soils from Matatirtha and Dhaksi ridges. Open triangle represents Atterberg limits of soils from selected site, whereas open circle represents Atterberg limits of soils from surrounding area of selected sites

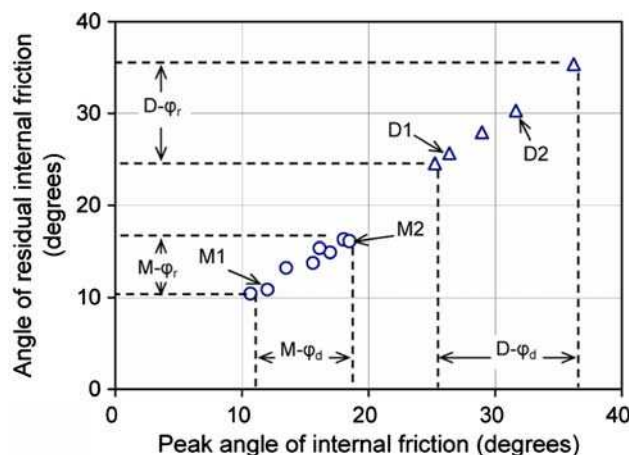


Fig. 9 Comparison of peak and residual angles of internal friction for representative soil samples from Matatirtha and Dhaksi ridges. The soil samples from sites M1, M2, D1, and D2 are also shown with open circle and open triangle notation

described by Geological Society Engineering Group Working Party (1977), the rock was moderately weathered. To understand the spatial orientation of joints sets, stereograms were used to represent the joint sets. The stereograms, along with the information about spacing and aperture, are given in Fig. 10. The cross sections of joint sets and a representative pattern of seepages are illustrated in Fig. 11. The topographical profiles in Fig. 11 were prepared nearly parallel to the strike of bedding joint, thus apparent dips of beds were used in cross section. Other joints were also plotted according to their apparent dips. The joint set 060°/55° (dip direction/dip) on Dhaksi ridge and joint set 026°/58° on Matatirtha ridge are parallel to the eastern slopes, and these sets were largely responsible for the seepage on slope during monsoon rainfall.

At the first visit to the study area, significant flows of water were noticed on the landslide scar and debris channel of the Matatirtha landslide (see Fig. 6). Moreover, seepage and springs were noticed on the uphill section during

**Table 1** Result of X-ray analysis of soils collected from both ridges and zero-order basins

Samples	Quartz	Feldspar	Illite	Smectite	Diaspore	Geothite	Calcite	Trace minerals
Matatirtha ridge	+++++	+++++	++	-	+	+	+	Smectite,boitite, wustite
	+++++	+++	++	+	+	-	+	Kaoline, biotite
	+++++	+++	+	++	+	-	+	Geothite, biotite
	+++++	++	++	+	+	-	+	Geothite, kaoline
	+++++	++	+	+	+	+	+	Kaoline, biotite, wustite
	+++++	+++	+	+	+	-	+	Geothite, wustite, kaoline
	+++++	+++	++	+	+	+	+	Kaoline, biotite
	+++++	+++	++	+	+	-	+	Geothite, kaoline
Dhaksi ridge	+++++	+	+	-	+	-	++	Kaoline, smectite, wustite
	+++++	+++	++	-	-	-	++	Smectite, wustite
	+++++	+++	++	+	+	+	+	Kaoline, biotite
	+++++	+++	++	-	+	-	+	Geothite, kaoline
	+++++	++	++	+	+	-	+	Geothite, kaoline, biotite
	+++++	++	++	-	+	+	+	Biotite, wustite, kaoline
	+++++	+++	++	-	+	-	+	Geothite, kaoline, wustite
	+++++	+++	++	-	+	-	+	Geothite, kaoline, wustite

Relative abundance: +++++ high ↔ + low

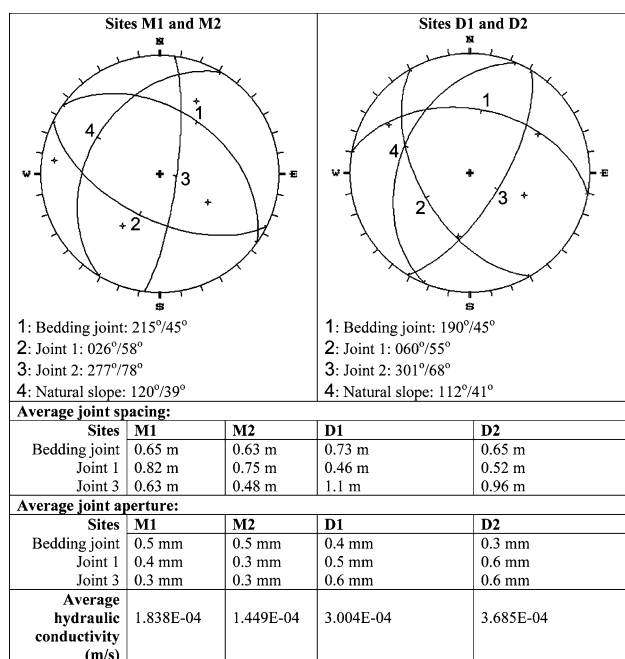


**Fig. 10** Data of rock joints on both ridges. Azimuth of natural slope and its inclination was selected according to profile line selected to prepare topographic profile illustrated in Fig. 11. Numbers in stereograms represent great circles of respective joints and slope. The joint data of 50 joints were used to determine the value of most representative joints. The stereographical projections are upper hemispherical projections

several of field visits. The role of bedrock fractures and ground water accumulation in relation to landslides and debris flows was well reviewed by Mathewson et al. (1990) in metamorphic and sedimentary terrains and by Onda

(2004) in granitic terrains. Wilson and Dietrich (1987) described the bedrock hydrology and pore pressure development in topographic hollows covered by colluvium. Therefore, the groundwater flow from fractures needs to be considered during the parameter study of landslides in the study area. Hence, the hydraulic conductivity of the bedrock was estimated according to theoretical method described by Goodman (1989). Equation 4 was used to estimate hydraulic conductivity of rock:

$$k = \frac{\gamma_w}{6m} \left( \frac{e^3}{S} \right) \tag{4}$$

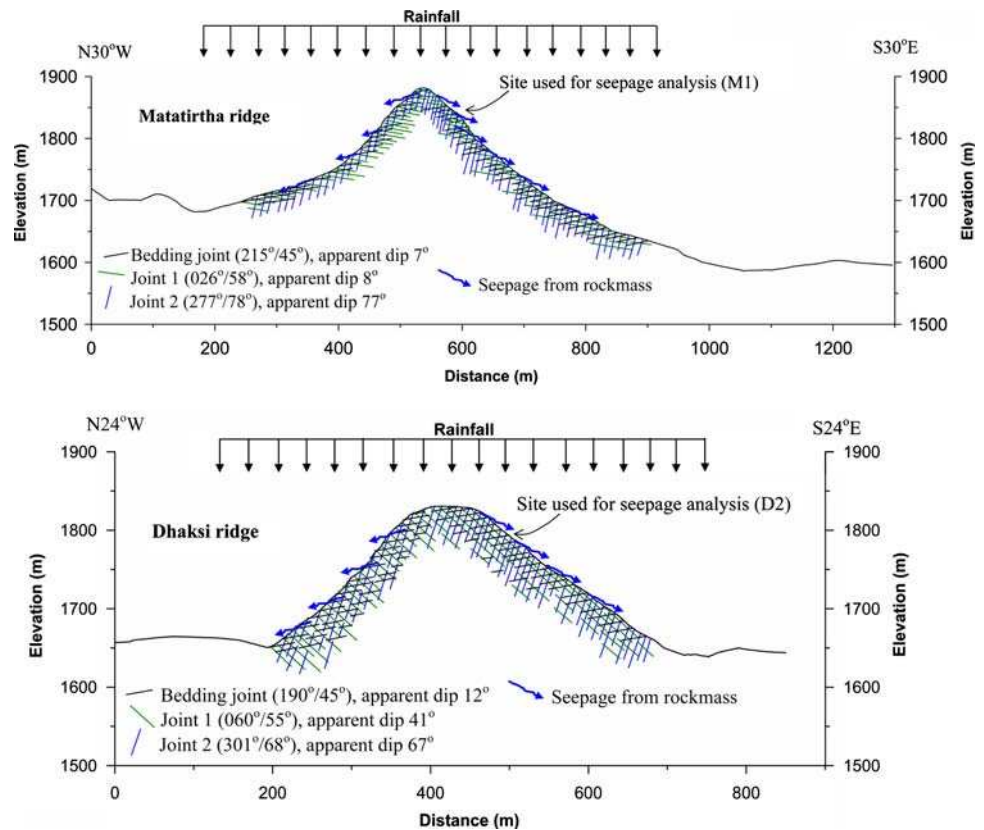
where  $k$  is hydraulic conductivity of the rockmass,  $\gamma_w$  is unit weight of water,  $\mu$  is viscosity of water,  $e$  is joint aperture or interwall separation, and  $S$  is joint spacing. Although Goodman (1989) described that Eq. 4 is useful for back calculation of aperture from in situ hydraulic permeability test data, in this study, data of joint aperture and spacing measured in the field were employed in Eq. 4 and rock hydraulic conductivity was estimated. The estimated average hydraulic conductivity of bedrock on Matatirtha and Dhaksi ridges are given in Fig. 10.

### Seepage and slope stability modeling

#### Model parameters

For the seepage and slope stability modeling in GeoStudio (2005), both laboratory and field data were used to assess the hydraulic properties of colluvial soils. Thickness of the colluvial layers were selected as per field measurements.

**Fig. 11** Illustration of joint patterns in rock on the two ridges. The attitudes of joints are in dip direction/dip format. Schematic representations of seepage are shown on both eastern and western slopes



Each zero-order configuration was modeled adopting slope angles measured in the field and slope lengths of 20 m. During modeling, all slopes were considered to be geometrically planar, having soil layers parallel to the ground surface. The parameters used in the models are illustrated in Table 2.

The volumetric water content functions and the hydraulic conductivity functions were obtained from curves derived using the algorithm of Green and Corey (1971) for soils with similar grain size distributions, adjusting the saturated water content and permeability values to the actual measured values. The main failure events occurred on 23rd July 2002, and it was difficult to describe the initial pressure distribution prior to the rainfall events because almost all

days of July have considerable rainfall and no data was available for pore pressure variation. Thus, the simulation was performed considering daily rainfall intensity beginning from 1st July 2002 as a start-up period, and the initial water table was defined above the bedrock with a maximum negative pore pressure of 10 kPa. These kinds of simulations of long start-up periods usually indurate the computed initial conditions (here, pore water pressure) and its effect in the main event is negligible (Reid et al. 1988).

Regarding the boundary conditions, a transient flux function with values equal to the daily rainfall rate for July 2002 was applied to the nodes along the ground surface. A null flux condition was assigned to the upslope and

**Table 2** Parameters used in simulations

Sites	USCS	Soil Thickness (m)	Slope angle (°)	Soil Cohesion (kN/m <sup>2</sup> )	Unit weight (kN/m <sup>3</sup> )	Friction angle (°)	Volumetric water content (%)	Saturated hydraulic conductivity of soil (m/s)	Hydraulic conductivity of rockmass (m/s)
M1	ML	1.41	31.0	4.6	15.64	27.6	46.0	2.241E-03	1.838E-04
M2	ML	0.90	33.0	12.6	14.00	27.5	47.0	2.349E-03	1.449E-04
D1	MH	1.25	28.0	5.9	13.80	30.4	51.0	3.150E-03	3.004E-04
D2	ML	1.20	26.0	4.1	14.80	30.6	48.0	6.389E-03	3.685E-04

Cohesion and friction angle were estimated by direct shear test, volumetric water content in saturation and unit weight were estimated in the lab. Soil hydraulic conductivity was measured in field. Hydraulic conductivity of rock was estimated from Goodman (1989)

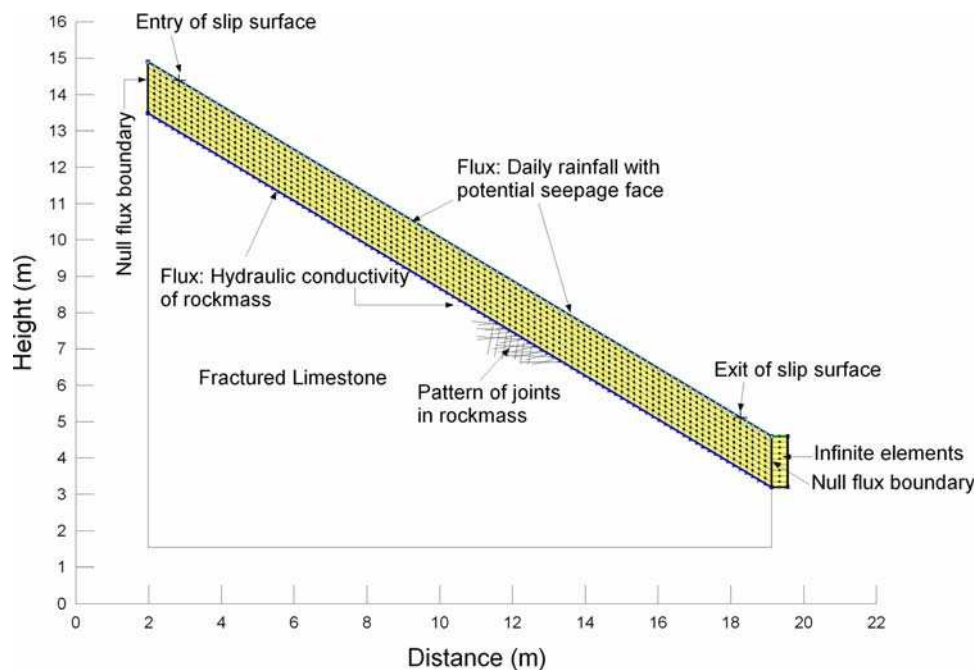
downslope vertical faces of the model. In the case of the downslope vertical face, the infinite elements option was also selected to extend the actual right edge to infinity in the positive  $x$ -direction, to avoid an unnatural impermeable border, and minimize any side effects. A semi transient flux condition with respect to estimated rate of hydraulic conductivity of limestone (Table 2) was imposed at the lower boundary of each simulation. This boundary is semi transient because, for the all days of July, the hydraulic conductivity of rock was considered to be zero except for the day of maximum rainfall (23 July 2002), when the values of estimated hydraulic conductivity of particular sites were considered in boundary flux. Regular field observations of existing springs and seepage in the surrounding area support this assumption. Moreover, flow of water observed on the debris flow channel of on 24 July 2002 (32 h after the landslide event) also supports the concept of this semi transient boundary flux. The complete layout of model is shown in Fig. 12.

Considering the entire month's rainfall for simulation without considering evaporation rate is an important limitation of this analysis. In reality, the actual evaporation or evapotranspiration rate from the surface is a function of vegetation cover, soil moisture, and sunlight hour. SEEP/W v.4 can handle an evaporative flux only by defining a negative flux along the ground surface. Thus, to incorporate evaporation as a negative flux in the seepage analysis, an average evaporation flux rate was applied along the surface during the preliminary phase of analysis. The result of pore pressure reduction, however, was very unrealistic in

comparison to the field problems. Other researchers have also had similar experiences during seepage analysis (Gasmo et al. 2000; Tsaparas et al. 2002). In general, during extreme monsoon rainfall events negligible evaporation takes place, and since this study is focusing on the changes in pore water pressures during extreme monsoon rainfall events, evaporation would not be a major limitation. Likewise, the temporal distribution of short-term rainfall intensity also affected landslide occurrence. In this simulation, due to lack of hourly rainfall data, only constant rainfall intensity for 24 h was used. This was another limitation of the modeling.

In modeling with SEEP/W, bedrock hydrology was not incorporated (e.g., Casagli et al. 2006; Dapporto et al. 2005; Crosta and Dal Negro 2003). However, the role of bedrock seepages in slope failures and debris flows is well described in the literature (Mathewson et al. 1990; Onda 2004; Wilson and Dietrich 1987). Therefore, to ascertain the applicability of bedrock seepage in modeling, site M1 (crown of Matatirtha landslide) was simulated with both scenarios of seepage through rock (M1 simulation) and no seepage through rock (M1NFB simulation), i.e., as a null flux boundary on soil-bedrock contact. For bedrock seepage, only the extreme rainfall period was considered as effective rainfall for groundwater flow. From the field observations of slopes from 2002 to 2006, the normal monsoon rainfalls (less than 100 mm per day) were not found to be effective for groundwater flow in the uphill section of the study area. However, such rainfalls were responsible for springs and seepages originating at the base

**Fig. 12** Configuration of model from site M1. The homogeneous colluvium above the bedrock was considered as single layer for modelling. The joints are plotted according to orientations measured in the field, and are described in Fig. 11. A null flux condition was assigned to the upslope and down slope vertical faces of the model



of the hills. In fact, such rains could not provide enough water for raising the groundwater table from downhill to uphill slope.

Five simulations (M1 and M1NFB as well as M2, D1, and D2) were performed dividing the monsoon rainfall event of July 2002 into 744 time steps of 1 h length (total 31 days).

Result of seepage analysis

The value of pore water pressure in each slope was usually high in 23 July, which was the date of failure of the Matatirtha landslide. The role of antecedent rainfall was almost negligible in all simulations. Pore water pressure development was usually transient because of the high permeability of soil and potential seepage faces on the slope. Pore water pressure variations in July at the optimized slip surface having lowest value of factor of safety are shown in Fig. 13. The optimized slip surfaces of each site are shown in Fig. 14 on the day of maximum rainfall

(23 July). The distribution of the water table varied in all five simulations. In simulation M1, many temporary saturated zones (perch water tables) developed within the soil stratum. The soil appeared almost saturated on the date of failure (Fig. 14). On the other hand, in simulation M1NFB, the soil strata were partly saturated. Similarly, few perched aquifers were noticed in simulations M2, D1, and D2 during the July rainfall, but on the day of failure, soil strata were usually found to be partly saturated. The differences of between simulations M1 (groundwater flow included) and M1NFB (groundwater flow not included) were mainly in the distribution of pore water pressure in the soil strata and the rise of the groundwater table.

Stability analysis and result

Slope stability analyses were conducted for each of the simulations used for seepage analysis, using pore water pressures determined at different time steps as input data for a limit equilibrium analysis performed with SLOPE/W

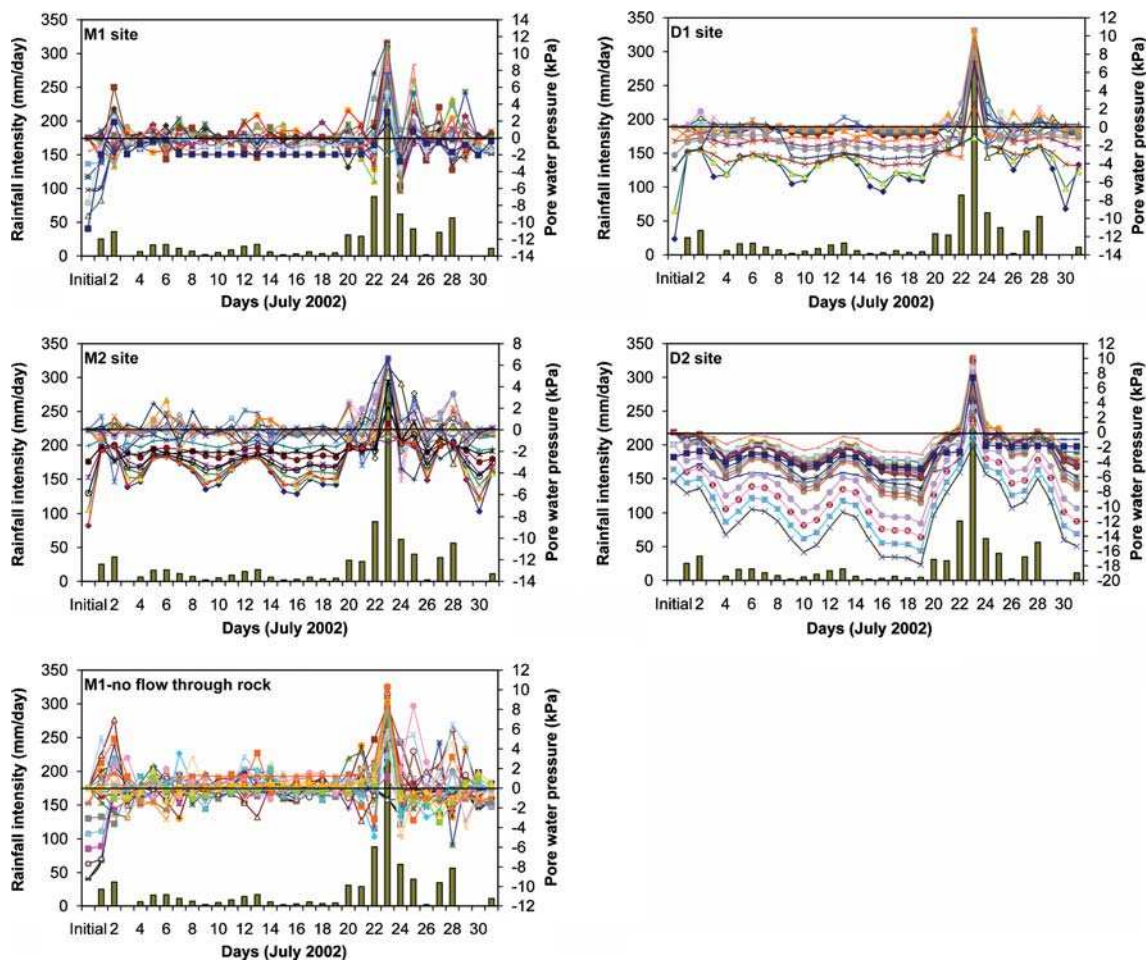
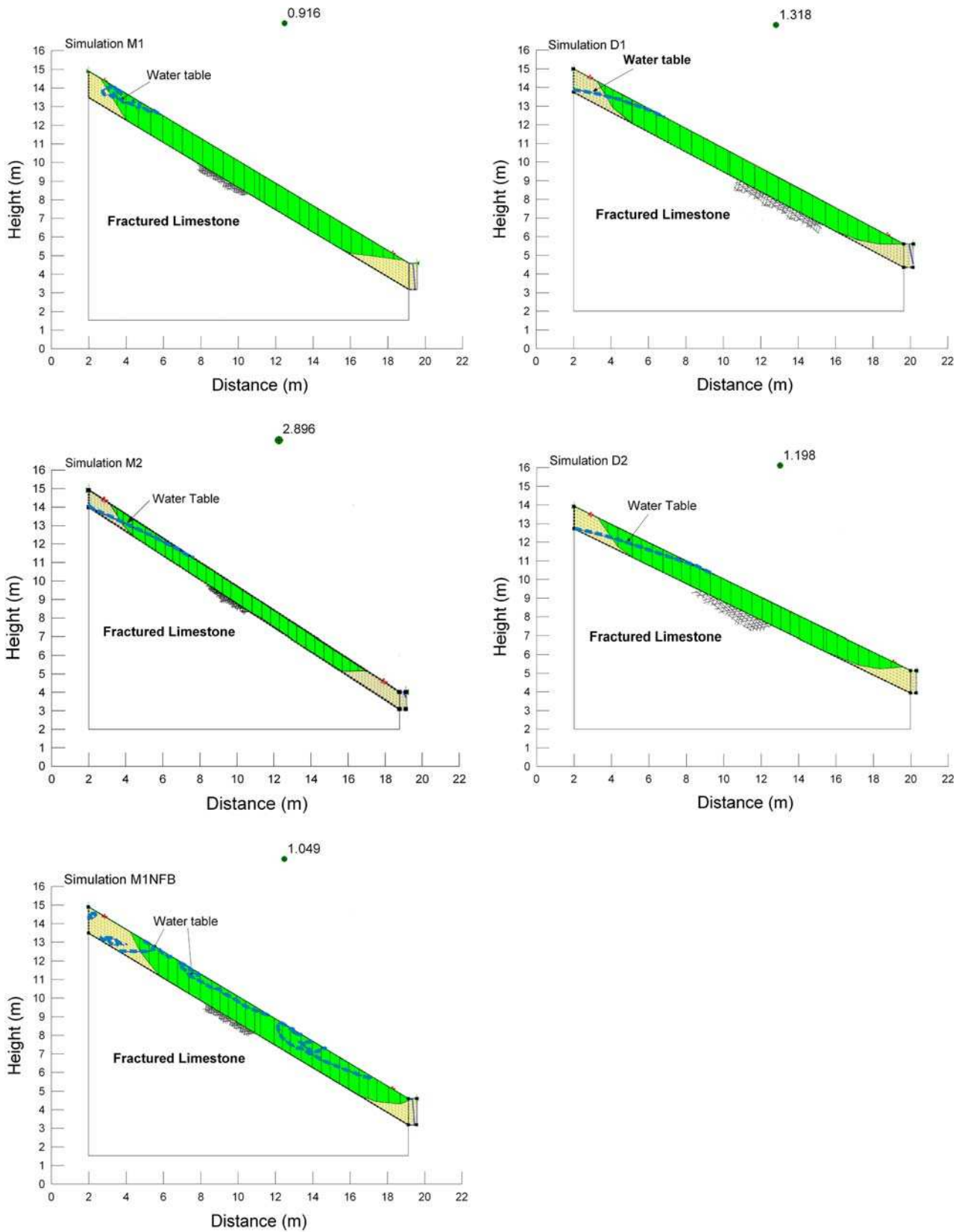


Fig. 13 Pore water pressure variation in July at the optimized slip surface having lowest factor of safety. The optimized slip surfaces were obtained for the day of maximum rainfall and are shown in Fig. 14 for each site



**Fig. 14** Result of slope stability analysis and optimized slip surface. The pore water pressure of 552 steps of the seepage analysis was used in this stability analysis

v.4 software (GeoStudio 2005). The factor of safety of the soil cover was computed with the Morgenstern–Price method. The ratio of shear strength to shear stress is called the factor of safety. When this ratio is greater than 1, shear strength is greater than shear stress and the slope is considered stable. When this ratio is close to 1, shear strength is nearly equal to shear stress and the slope is unstable.

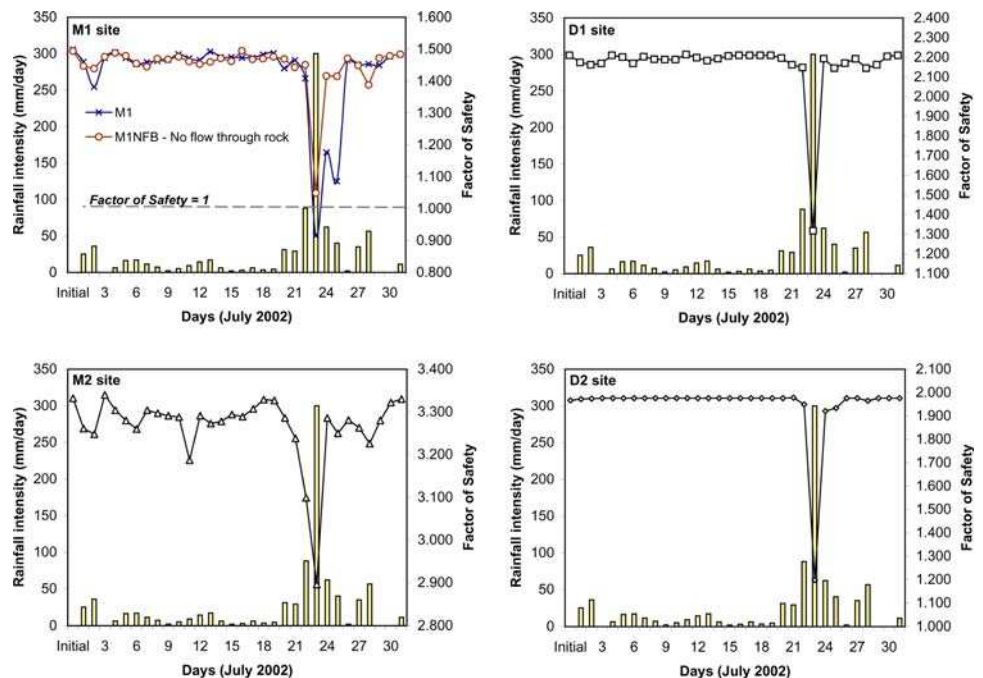
The geotechnical parameters adopted for all selected sites are already reported in Table 2, and they were decided from precise field and laboratory investigations. In each model, an entry and exit type (GeoStudio 2005) critical slip surface was considered at a surface distance of 1 m from the upslope edge and downslope edge (see Fig. 12). During the stability analysis, critical slip surfaces were optimized with a maximum of 2,000 iterations. The optimized slip surfaces were estimated from each model for the month of July. The optimized critical slip surfaces and respective factors of safety on the date of failure on Matatirtha ridge are illustrated in Fig. 14. In all simulations, factors of safety decreased abruptly on the date of maximum rainfall. At the date of failure, the factor of safety at site M1 was less than 1, whereas for other sites it was more than 1. For the same site, stability analysis was also conducted from the pore water pressure data of the M1NFB simulation. The optimized factor of safety could not reach below 1 even with an effective cohesion value of 4.6 kN/m<sup>2</sup>, and the resulting failure block was also smaller than that of simulation M1. The variations of factor of safety in each modeling scenario in the month of July are shown in Fig. 15.

Discussions

In this paper, a comprehensive geological, geomorphological, and geotechnical investigation is discussed to understand the contributing parameters involved in landslide triggered by extreme monsoon rainfall in the Lesser Himalaya by comparing a non-landslide zone and a landslide-prone zone. In this study, various experiments were conducted to ascertain the effective contributing parameters for landslides in the Lesser Himalaya.

The X-ray diffraction study confirmed that the soil consists of quartz, feldspar, and illite as major constituent minerals, along with significant amounts of smectite, kaolinite, calcite, and iron minerals. Large amounts of quartz in the soil imply that the soil is in a later stage of weathering after its deposition in the geological past. The presence of illites in the slope materials was the main cause of low frictional resistance obtained by ring shear test. Smectite was also noticed in the soil from X-ray analysis. When such swelling minerals are present in slope materials, the slopes are prone to failure. Swelling minerals such as smectites expand when they become wet as water enters the crystal structure and increases the volume of the mineral. During heavy rainfall, they swell and slopes become prone to failure. Previous studies involving the role of swelling clay minerals in activating a landslide have shown that even a small amount of swelling clay minerals in soil greatly affects its strength behavior. Kerr (1972) highlighted the role of clay minerals in landslide formation and described the effect on velocity in landslide movement.

Fig. 15 Change of factor of safety with rainfall in July 2002. For site M1, two scenarios of pore water pressure were used for stability analysis, and the factor of safety calculated from M1NFB could not reach below the critical value



Bardou et al. (2004) noticed a dramatic change in rheological parameters when small changes occurred in the swelling clay ratio (SCR) of the debris materials. Similarly, Yatabe et al. (2000) found that an increase in the relative amount of swelling clay minerals in landslide materials results in a decrease of angle of shearing resistance, as illustrated in Fig. 16 (Yatabe et al. 2000). Swelling clay ratio (SCR) represents the relative amount of swelling clay minerals in the tested samples, as estimated from X-ray diffraction patterns. In the study area, the amount of smectite is comparatively high in site M1 (Matatirtha landslide site, see Table 1). Thus, the presence of swelling minerals in the slope materials of the study area greatly supports the occurrence of landslides in the Matatirtha ridge.

The bedrock geology of the study area is mainly fractured limestone, and on the base of hills villagers use spring water for daily use. Solution activities in limestone facilitate remarkable ground water percolation within the bedrock. Hydraulic conductivity of the rock estimated in this paper by the method proposed by Goodman (1989) suggested saturated flow through the rock mass is possible with a conductivity of  $10^{-4}$  m/s. The orientation of joints in the slope also supports water flow through rock during extreme rainfall events, and such flow was observed during first field visit. The colluvial soil above the bedrock mainly consists of silty clay with fine sand. In situ measurements of infiltration capacity of soils revealed that the soils are relatively permeable and have conductivity rates in the range of  $10^{-3}$  m/s. The colluvium is well vegetated by shallow rooted vegetation, is relatively loose, and its bulk density is low. Thus, rainwater can easily infiltrate within the soil. In the extreme rainfall events of 2002, rainfall recharged the fractures in the bedrock and immediately a

shallow ground water system was established and maintained in the colluvium through ground water seepage from bedrock. Thus, bedrock hydrogeology is another contributing factor for landsliding in the study area.

The thickness of colluvium in zero-order basins is also relatively high. On the scar of the Matatirtha landslide, the average soil thickness was 1.5 m. This thickness on uphill slopes (average inclination  $28^{\circ}$ – $42^{\circ}$ ) of zero-order basins is found to be very favorable for landsliding.

The study area consists of two types of ridge in the context of landslide occurrence. Landslides were concentrated on Matatirtha ridge only and there are no landslides in Dhaksi ridge although both have the same geological and geomorphological setting. To evaluate the strength of the soil on both ridges, four sites were selected for detail study and soil samples were investigated in the lab. From the Bishop type ring shear test, it was found that Matatirtha ridge has fine soils (grain size less than 0.425 mm) having lower residual strength than those on Dhaksi ridge. The effective shear strengths estimated from constant pressure direct shear tests (soil grain size less than 2 mm) are also less than on Dhaksi ridge. We conclude that the low shear strength of the fines in the soils is another contributing factor for landsliding.

After understanding geological and geomorphological setting of area as well as geotechnical properties of slope materials, seepage modeling, and stability analysis were performed using the GeoStudio (2005) computer application to understand the relationship of pore water pressure and stability of soil layers during rainfall. Because hourly rainfall data were unavailable, daily rainfall data were used in the simulations. Varied transient pore water pressure with respect to rainfall was observed in the simulated slopes. The stability analysis of the simulated slope showed a minimum factor of safety on 23 July 2002, but among the selected four sites, only the Matatirtha landslide site possessed a factor of safety less than 1 by maintaining simulated slip surface at bedrock and colluvium contact. In the real event, the colluvium layer was completely removed from the slope. Thus the modeling was significant and accurately represented the real scenario. Likewise, the consideration of bedrock seepage during extreme rainfall events could demonstrate the modeling in a real sense. The result of the slope stability analysis without considering bedrock would not accurately model the real scenario. In many cases, the same rainfall influenced landslide initiation differently depending on site characteristics and soil thickness. Short-term intensity and temporal distribution of rainfall largely influenced the landslide occurrence. But in the case of the Nepal Himalayan slopes, temporal variation and short-term intensity of rainfall is hard to interpret due to lack of rainfall data. This study thus attempted to use daily rainfall to model rainfall and landslide relationships.

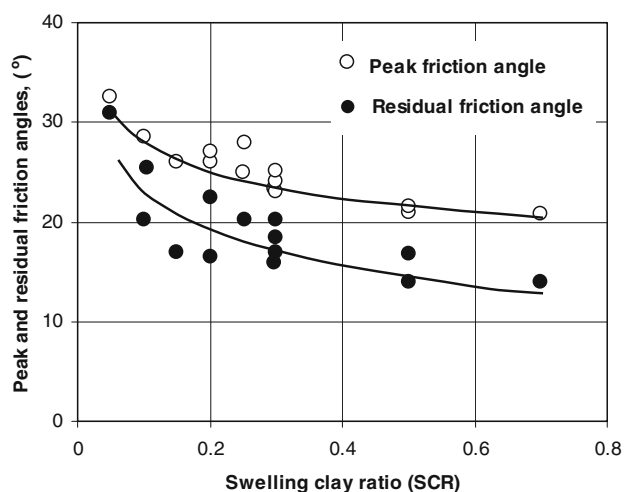


**Fig 16** Variations of strength of landslide soil with increasing amount of swelling clay minerals (after Yatabe et al. 2000)

For the first time, the transient pore water pressure and factor of safety variations in the Lesser Himalayan slopes during extreme events of monsoon rainfall were well understood from this modeling. In general, slopes with lower hydraulic conductivity are most prone to shallow failures due to the significant pore water pressure response to the rainfall, which leads to the considerable loss of soil suction and rise of positive pore water pressure under moderately intense rainfall. In contrast, under the same rainfall condition, slopes with high hydraulic conductivity tend to remain stable due to the slight pore water pressure response to rainfall. They require more intensive and longer duration rainfall for landsliding. The hydraulic conductivity rate of slope materials in the study area was in the range of  $10^{-3}$  to  $10^{-4}$  m/s. This is a moderate hydraulic conductivity for soil. Therefore, high intensity (average 24-h rainfall of 12.5 mm/h) and continuous rainfall from the morning of 22 July to the morning of 23 July 2002 was the main responsible rainfall for landsliding in the study area.

To explore the contributing factors for landslides, many parameters were investigated in this study for a relatively small area. However, this methodology can be replicated over a wide area, for example, over a catchment having an area of 5–10 km<sup>2</sup>. For this purpose, special attention should be given to separate small topographic units having more or less similar geomorphologic characteristics. In the Lesser Himalaya of Nepal, separation of such topographic units is possible from available topographic maps and reconnaissance field studies. Representative soil sampling, in situ tests and rock exposure studies in each unit assist in separating topographic units of similar geotechnical and geological characters. Seepage as well as stability analysis in two or three representative topographic units having different geological and geotechnical characters will allow upscaling of this research to a larger area.

## Conclusions

The following concluding remarks can be drawn by this study.

- Soil characteristics, low internal friction angle of fines in soil, the presence of clay minerals, bedrock hydrology, and human intervention (road construction) were the main contributing parameters for slope failures on Matatirtha ridge.
- There is a spatial variation of landslide occurrences owing to soil characteristics, high internal friction angle of fines in the soils, and less soil thickness.
- The clay mineralogy of slope materials is also a contributing factor for rainfall-triggered landslides in the Lesser Himalaya.

- By modeling pore water pressure and slope stability in the non-landslide zone and the landslide-prone zone, we found that shallow and highly mobile landslides in zero-order basins or topographic hollows of Lesser Himalayan slopes are mainly triggered by transient positive pore water pressure in response to intense monsoon rainfall and bedrock seepage. This is the first time this kind of modeling has been performed for the Lesser Himalayan slopes of Nepal and it needs to be carried out for other slopes with multiple layers of colluvial deposits and a wide range of geotechnical properties.
- The role of bedrock hydrogeology is another promising subject that requires study as a factor in rainfall-triggered landslides in the region.
- Antecedent rainfall affects landslide stability by reducing soil suction and increasing transient pore water pressure. The recent study of Dahal and Hasegawa (2008) on landslide and monsoon rainfall concluded that there was a significant role of antecedent rainfall in the Nepal Himalaya especially in the northeastern part of central Nepal, and such rainfall was basically responsible for large scale landsliding. Seepage analysis of antecedent rainfall in the study area (middle part of central Nepal) has shown slight effects on buildup of pore water pressure on the slope. Thus, in the Lesser Himalaya of central Nepal, extreme rainfall of 1 or 2 days is usually responsible for shallow slope failures.
- When topographic units having similar geomorphologic characteristics are separated, this research can be replicated over a larger geographic area.

**Acknowledgments** The authors would like to thank relatives of victims of the Matatirtha landslide for their cooperation in field investigations. We are grateful to M.Sc. students (2002 batch) of the Central Department of Geology, Tribhuvan University, for providing help in field work. We thank Mr. Pradeep Paudyal, Mr. Amar Chand, Mr. Kangada Prasai and Mr. Hari Kadel for their help in the collection of field data. We also acknowledge local community forest user groups for providing permission to enter the forest for investigation. We thank Mr. Bhoj Raj Pantha, Mr. Anjan Kumar Dahal and Ms. Seiko Tsuruta for their technical support during the preparation of this paper. The study was partially funded by the Sasakawa Fund for Scientific Research, The Japan Science Society.

## References

- Aleotti P (2004) A warning system of rainfall-induced shallow failure. *Eng Geol* 73:247–265
- Anderson MG, Lloyd DM (1991) Using a combined slope hydrology-stability model to develop cut slope design charts. *Proc Inst Civil Eng* 91:705–718
- Anderson SA, Sitar N (1995) Analysis of rainfall-induced debris flows. *ASCE J Geotech Eng* 121(7):544–552

- ASTM D3385-03 (2003) Standard test method for infiltration rate of soils in field using double-ring infiltrometer, ASTM International, 100 Bar, harbor Drive, west Conshohocken, 19428
- Bardou E, Bowen P, Banfill PG, Boivin P (2004) Dramatical impact of low amounts of swelling clays on the rheology of alpine debris flows. *Eos Trans AGU* 85(47), Fall Meet (Suppl), Abstract H41B-0293
- Beven KJ, Kirkby MJ (1979) A physical based variable contributing area model of basin hydrology. *Hydrol Sci Bull* 24(1):43–69
- Bhandary NP, Yatabe R (2007) Ring shear tests on clays of fracture zone landslides and clay mineralogical aspects. In: Sassa K, Fukuoka H, Wang F, Wang G (eds) *Landslide risk and sustainable disaster management. Proceeding of first general assembly of Internal Consortium on Landslides*. Springer, Germany, pp 183–192
- Bishop AW, Green GE, Garga VK, Andresen A, Brown JD (1971) A new ring shear apparatus and its application to the measurement of residual strength. *Géotechnique* 21(4):273–328
- Borga M, Dalla FG, Gregoretti C, Marchi L (2002) Assessment of shallow landsliding by using a physically based model of hillslope stability. *Hydrol Processes* 16:2833–2851
- Brand EW, Permechitt J, Phillison HB (1984) Relationship between rainfall and landslides in Hong Kong. *Proc 4th Int Symp Landslides* 1:377–384
- Cai F, Ugai K (2004) Numerical analysis of rainfall effects on slope stability. *Int J Geomech* 4:69–78
- Caine N (1980) The rainfall intensity-duration control of shallow landslides and debris flows. *Geografiska Annaler* 62A:23–27
- Campbell RH (1975) Soil slips, debris flows, and rainstorms in the Santa Monica Mountains and vicinity, Southern California. U S Geological Survey Professional Paper 851:1–20
- Casagli N, Dappoorto S, Ibsen ML, Tofani V, Vannocci P (2006) Analysis of the landslide triggering mechanism during the storm of 20th–21st November 2000, in Northern Tuscany. *Landslides* 3:13–21
- Collins BD, Znidarcic D (2004) Stability analyses of rainfall induced landslides. *J Geotech Geoenviron Eng* 130:362–372
- Collison AJC, Anderson MG (1996) Using a combined slope hydrology/slope stability model to identify suitable conditions for landslide prevention by vegetation in the humid tropics. *Earth Surface Processes Landforms* 21:737–747
- Crosta GB, Dal Negro P (2003) Observations and modelling of soil slip-debris flow initiation processes in pyroclastic deposits: the Sarno 1998 event. *Nat Hazards Earth Sys Sci* 3:53–69
- Crozier MJ (1999) Prediction of rainfall-triggered landslides: a test of the antecedent water status model. *Earth Surface Processes Landforms* 24:825–833
- Dahal RK, Hasegawa S (2008) Representative rainfall thresholds for landslides in the Nepal Himalaya. *Geomorphology* 100(3–4):429–443
- Dahal RK, Kafle KR (2003) Landslide triggering by torrential rainfall, understanding from the Matatirtha landslide, south western outskirts of the Kathmandu valley. In: *Proceedings of one day International seminar on Disaster mitigation in Nepal*, Nepal Engineering College and Ehime University, pp 44–56
- Dahal RK, Hasegawa S, Yamanaka M, Nishino K (2006) Rainfall triggered flow-like landslides: understanding from southern hills of Kathmandu, Nepal and northern Shikoku, Japan. *Proc 10th Int Congr of IAEG, The Geological Society of London, IAEG2006 Paper number 819:1–14 (CD-ROM)*
- Dahal RK, Hasegawa S, Nonomura A, Yamanaka M, Masuda T, Nishino K (2008a) Failure characteristics of rainfall-induced shallow landslides in granitic terrains of Shikoku Island of Japan. *Env Geol*, online first. doi:10.1007/s00254-008-1228-x
- Dahal RK, Hasegawa S, Nonomura A, Yamanaka M, Dhakal S (2008b) DEM based deterministic landslide hazard analysis in the Lesser Himalaya of Nepal. *Georisk* (in press). doi:10.1080/17499510802285379
- Dahal RK, Hasegawa S, Nonomura A, Yamanaka M, Dhakal S, Paudyal P (2008c) Predictive modelling of rainfall-induced landslides hazard in the Lesser Himalaya of Nepal based on weights-of-evidence. *Geomorphology* (in press). doi:10.1016/j.geomorph.2008.05.041
- Dai F, Lee CF, Wang SJ (1999) Analysis of rainstorm-induced slide-debris flows on natural terrain of Lantau Island, Hong Kong. *Eng Geol* 51:279–290
- Dappoorto S, Aleotti P, Casagli N, Polloni G (2005) Analysis of shallow failures triggered by the 14–16 November 2002 event in the Albaredo valley, Valtellina (Northern Italy). *Adv Geosci* 2:305–308
- De Prete M, Guadagno FM, Hawkins AB (1998) Preliminary report of the landslides of 5 May 1998, Campania, southern Italy. *Bull Eng Geol Env* 57:113–129
- Dhakal AS, Sidle RC (2004) Distributed simulations of landslides for different rainfall conditions. *Hydrol Processes* 18:757–776
- Dhital MR (2003) Causes and consequences of the 1993 debris flows and landslides in the Kulekhani watershed, central Nepal. In: Rickenmann D, Chen C-L (eds) *Proceedings of 3rd International Conference Debris-Flow Hazards Mitigation: mechanics, prediction and assessment, vol 2*. Millpress, Rotterdam pp 931–942
- Dhital MR, Khanal N, Thapa KB (1993) The role of extreme weather events, mass movements, and land use changes in increasing natural hazards, a report of the preliminary field assessment and workshop on causes of recent damage incurred in south-central Nepal, 19–20 July 1993. *ICIMOD, Kathmandu*, p 123
- Dietrich WE, Reiss R, Hsu M, Montgomery DR (1995) A process-based model for colluvial soil depth and shallow landsliding using digital elevation data. *Hydrol Processes* 9:383–400
- Dunne T (1978) Field studies of hillslope flow processes. In: *Hillslope Hydrology*, Kirkby MJ, (eds.). Wiley, Chichester, pp 227–293
- Ellen SD, Fleming RW (1987) Mobilization of debris flows from soil slips, San Francisco Bay region, California. In: Costa JE, Wieczorek GF (eds) *Debris flows/avalanches: process, recognition, and mitigation, vol 7*. Geological Society of American Review Engineering Geology, Boulder pp 31–40
- Fannin RJ, Jaakkola J (1999) Hydrologic response of hillslope soils above a debris-slide headscarp. *Can Geotech J* 36:111–1122
- Fredlund DG, Morgenstern NR (1976) Constitutive relations for volume change in unsaturated soils. *Can Geotech J* 13:261–276
- Fredlund DG, Morgenstern NR (1977) Stress state variable for unsaturated soils. *ASCE* 103:447–464
- Fredlund DG, Rahardjo H (1993) *Soil mechanics for unsaturated soils*. Wiley, New York, p 517
- Gasmo JM, Rahardjo H, Leong EC (2000) Infiltration effects on stability of a residual soil slope. *Comp Geotech* 26(02):145–165
- Geological Society Engineering Group Working Party (1977) *The description of rock masses for engineering geology*. *Eng Geol* 10(4):355–388
- GeoStudio (2005) *GeoStudio Tutorials includes student edition lessons*, 1st edn. Geo-Slope International Ltd., Calgary
- Giannecchini R (2006) Relationship between rainfall and shallow landslides in the southern Apuan Alps (Italy). *Nat Hazards Earth Sys Sci* 6:357–364
- Glade T, Crozier M, Smith P (2000) Applying probability determination to refine landslide-triggering rainfall thresholds using an empirical Antecedent Daily Rainfall Model. *Pure Appl Geophys* 157:1059–1079
- Goodman RE (1989) *Introduction to rock mechanics*, Wiley, New York, 562p
- Green RE, Corey JC (1971) Calculation of hydraulic conductivity: a further evaluation of some predictive methods. *Soil Sci Soc Am* 35:3–8

- Guadagno FM, Celico PB, Esposito L, Perriello ZS, Piscopo V, Scarascia-Mugnozza G (1999) The Debris Flows of 5–6 May 1998 in Campania, Southern Italy. *Landslide News* 12:5–7
- Guzzetti F, Cardinali M, Reichenbach P, Cipolla F, Sebastiani C, Galli M, Salvati P (2004) Landslides triggered by the 23 November 2000 rainfall event in the Imperia Province, Western Liguria, Italy. *Eng Geol* 73:229–245
- Hasegawa S, Dahal RK, Yamanaka M, Bhandary NP, Yatabe R, Inagaki H (2008) Causes of large-scale landslides in the Lesser Himalaya of central Nepal. *Environ Geol* (Accepted)
- Hennrich K, Crozier MJ (2004) A hillslope hydrology approach for catchment-scale slope stability analysis. *Earth Surf Process Landforms* 29:599–610
- Hungr O (1995) A model for the run out analysis of rapid flow slides, debris flows and avalanches. *Can Geotech J* 32:610–623
- Hungr O (2003) Flow slides and flows in granular soils. In: *Proceedings of international workshop on occurrence and mechanisms of flows in Natural Slopes and Earth fills*, electronic copy in web site. <http://www.unina2.it/flows2003/flows2003/articoli/Hungr-Flows.pdf>, p 9
- Hungr O, Morgan GC, Kellerhals R (1984) Quantitative analysis of debris torrent hazards for design of remedial measures. *Can Geotech J* 21:663–677
- Iverson RM (1997) The physics of debris flows. *Rev Geophys* 5:245–296
- Iverson RM (2000) Landslide triggering by rain infiltration. *Water Resour Res* 36(7):1897–1910
- Iverson RM, Reid ME, La Husen RG (1997) Debris-flow mobilization from landslides. *Annu Rev Earth Planet Sci* 25:85–138
- JICA (1993) Report of Japan Disaster Relief Team (Expert Team) on heavy rainfall and floods in Nepal, Japan International Cooperation Agency (JICA), JR1JDC/93-03, unpublished 125p
- Kerr PF (1972) The influence of clay minerals on surficial earth movements, Final report. Department of Geology, Columbia University, New York, 24 p
- Kim J, Jeong S, Park S, Sharma J (2004) Influence of rainfall-induced wetting on the stability of weathered soils slopes. *Eng Geol* 75:251–262
- Krahn J (2004a) Seepage modeling with SEEP/W, an engineering methodology, 1 th edn. Geo-Slope International Ltd, Alberta
- Krahn J (2004b) Stability modeling with SLOPE/W, an engineering methodology, 1st edn. Geo-Slope International Ltd., Calgary
- Lamb R, Beven KJ, Myrabo S (1998) A generalized topographic-soil hydrological index. In: Lane S, Richard K, Chandler J (eds) *Landform monitoring, modelling and analysis*. Wiley, Chichester, pp 263–278
- Lan H, Zhou C, Lee CF, Wang S, Wu F (2003) Rainfall induced landslide stability analysis in response to transient pore pressure—a case study of natural terrain landslide in Hong Kong, *Science in China Ser. E Technological Sciences* 46 (Suppl), pp 52–68
- Li T (1990) Landslide management in the mountain area of China, ICIMOD Kathmandu, Occasion Paper no. 15, p 50
- Lupini JF, Skinner AE, Vaughan PR (1981) The drained residual strength of cohesive soils. *Géotechnique* 31(2):81–213
- Mathewson CC, Keaton JR, Santi PM (1990) Role of bedrock ground water in the initiation of debris flows and sustained postflow stream discharge. *Bull Assoc Eng Geol* 27(1):73–83
- Montgomery DR, Dietrich WE (1994) A physical based model for the topographic control on shallow landsliding. *Water Resour Res* 30(4):1153–1171
- Montgomery DR, Dietrich WE, Torres R, Anderson SP, Heffner JT, Loague K (1997) Hydrologic response of a steep unchanneled valley to natural and applied rainfall. *Water Resour Res* 33(1):91–109
- NRCS (2008) Situation monitoring report of disaster (covering 15 June to 2 September 2008). Disaster Management Department, Nepal Red Cross Society, Kathmandu, Nepal (unpublished)
- Olivares L, Picarelli L (2003) Shallow flowslides triggered by intense rainfalls on natural slopes covered by loose unsaturated pyroclastic soils. *Géotechnique* 53(2):283–287
- Onda Y (2004) Hillslope hydrology and mass movements in the Japanese Alps. In: Owens PN, Slaymaker O (ed) *Mountain Geomorphology*, pp 153–164
- Pack RT, Tarboton DG, Goodwin CN (1998) SINMAP, A stability index approach to terrain stability hazard mapping, Users Manual (available at <http://www.tclbc.com>), Utah State University, Terratech Consulting Ltd., Canadian Forest Products Ltd, CN Goodwin Fluvial System Consulting, p 68
- Pack RT, Tarboton DG, Goodwin CN (2001) SINMAP approach to terrain stability mapping. In: Moore DP and Hungr O (eds) *Proceedings of International Conference of International Association for Engineering Geology and the Environment*, AA Balkema, Rotterdam, pp 1157–1165
- Paudel PP, Omura H, Kubota T, Morita K (2003) Landslide damage and disaster management system in Nepal. *Disaster Prevent Manage* 12(5):413–419
- Paudyal P, Dhital MR (2005) Landslide hazard and risk zonation of Thankot–Chalnakhel area, central Nepal. *J Nepal Geol Soc* 31:43–50
- Rahardjo H, Lim TT, Chang MF, Fredlund DG (1995) Shear strength characteristics of a residual soil. *Can Geotech J* 32:60–77
- Rahardjo H, Leong EC, Rezaur RB (2002) Studies of rainfall-induced slope failures. In: Paulus P, Rahardjo H (eds) *Slope 2002. Proceedings of the National Seminar, Slope 2002. 27 April 2002, Bandung*, pp 15–29
- Rahardjo H, Lee TT, Leong EC, Rezaur RB (2005) Response of residual soil slope to rainfall. *Can Geotech J* 42(2):340–351
- Reid ME, Nielson HP, Dreiss SJ (1988) Hydrologic factors triggering a shallow hillslope failure. *Bull Assoc Eng Geol* 25:349–361
- Rezaur RB, Rahardjo H, Leong EC (2002) Spatial and temporal variability of pore-water pressures in residual soil slopes in a tropical climate. *Earth Surf Processes Landforms* 27(3):317–338
- Richards LA (1931) Capillary conduction of liquids through porous mediums. *Physics* 1:318–333
- Rinaldi M, Casagli N (1999) Stability of streambanks formed in partially saturated soils and effects of negative pore water pressures: the Sieve River (Italy). *Geomorphology* 26:253–277
- Rinaldi M, Casagli N, Dapporto S, Gargini A (2004) Monitoring and modelling of pore water pressure changes and riverbank stability during flow events. *Earth Surf Process Landforms* 29:237–254
- Sassa K (1998) Recent urban landslide disasters in Japan and their mechanisms. In: *Proceedings of 2nd International Conference on Environmental Management, “Environmental Management”, Australia, 10–13 February, vol 1. Elsevier, Amsterdam*, pp 47–58
- Stark TD, Eid HT (1994) Drained residual strength of cohesive soils. *J Geotech Eng* 120(5):856–871
- Stöcklin J (1980) Geology of Nepal and its regional frame. *J Geol Soc London* 137:1–34
- Stöcklin J, Bhattarai KD (1977) Geology of Kathmandu Area and Central Mahabharat Range Nepal Himalaya Kathmandu. HMG/UNDP Mineral Exploration Project, Technical Report, New York, p 64
- Tika TE, Hutchinson JN (1999) Ring shear tests on soil from the Vaiont landslide slip surface. *Géotechnique* 49(1):59–74
- Tofani V, Dapporto S, Vannocci P, Casagli N (2006) Infiltration, seepage and slope instability mechanisms during the 20–21 November 2000 rainstorm in Tuscany, central Italy *Nat. Hazards Earth Sys Sci* 6:1025–1033

- Tsaparas I, Rahardjo H, Toll DG, Leong EC (2002) Controlling parameters for rainfall-induced landslides. *Comp Geotech* 29:1–27
- Tsuboyama Y, Sidle RC, Noguchi S, Murakami S, Shimizu T (2000) A zero-order basin—its contribution to catchment hydrology and internal hydrological processes. *Hydrol Process* 14(3):387–401
- Tsukamoto Y, Ohta T, Noguchi H (1982) Hydrological and geomorphological studies of debris slides on forested hillslopes in Japan. *Int Assoc Hydrol Sci Publication* 137:89–98
- Upreti BN (1999) An overview of the stratigraphy and tectonics of the Nepal Himalaya. *J Asian Earth Sci* 17:577–606
- Upreti BN, Dhital MR (1996) Landslide studies and management in Nepal. *ICIMOD*, p 87
- Van Genuchten MT (1980) A closed-form equation for predicting the hydraulic conductivity of unsaturated soils. *Soil Sc Soc Am J* 48:703–708
- Wagner A (1983) The principal geological factors leading to landslide in the foothills of Nepal: a statistical study of 100 landslides—steps for mapping the risk of landslides, HELVETAS-Swiss Technical Cooperation and ITECO-Company for International Cooperation and Development, unpublished, p 58
- Wang G, Sassa K, Fukuoka H (2003) Downslope volume enlargement of a debris slide-debris flow in the 1999 Hiroshima, Japan, rainstorm. *Eng Geol* 69:309–330
- Wang G, Sassa K, Fukuoka H, Tada T (2007) Experimental Study on the shearing behavior of saturated silty soils based on ring-shear Tests. *J Geotech Geoenv Eng* 133(3):319–333
- Wieczorek GF (1987) Effect of rainfall intensity and duration on debris flows in central Santa Cruz Mountains, California. *Geol Soc Am Rev Eng Geol* 7:93–104
- Wilson CL, Dietrich WE (1987) The contribution of bedrock groundwater flow to storm runoff and high pore pressure development in hollows, in *Erosion and Sedimentation in the Pacific Rim: International Association of Scientific Hydrology (IAHS) publication No. 165*, pp 49–59
- Wilson RC, Wieczorek GF (1995) Rainfall threshold for the initiation of debris flow at La Honda, California. *Env Eng Geosci* 1(1):11–27
- Yatabe R, Yagi N, Yokota K, Bhandary NP (2000) Influence of expansive chlorite on the strength of weathered Green Rock at Mikabu Belt of Japan, *Proceedings of International Conference on Geotechnical and Geological Engineering*, Melbourne, Australia, 19–24 November 2000 (CD format)